Inverse Problems **25** (2009) 045011 (21pp) doi:10.1088/0266-5611/25/4/045011

Robust determination of thermal diffusivity values from periodic heating data

L Perez[1] **and L Autrique**[2]

[1] Laboratoire de Thermocinétique de Nantes, Rue Christian Pauc, La Chantrerie, BP 50609, 44306 Nantes Cedex 3, France
[2] LISA, ISTIA, 62 Avenue Notre Dame du Lac, 49000 Angers, France

E-mail: laetitia.perez@univ-nantes.fr and laurent.autrique@univ-angers.fr

Received 31 March 2008, in final form 21 January 2009
Published 20 February 2009
Online at stacks.iop.org/IP/25/045011

Abstract

In this paper, an experimental technique dedicated to thermal diffusivity or thermal conductivity identification in isotropic and orthotropic materials is investigated. A method based on the analysis of thermal waves induced by periodic excitation in planar samples is proposed. Either frequency sweep at a single point in space or spatial fluctuations at a single frequency are considered. In such a context, in order to state both the accuracy and robustness of the data manipulation, a complete mathematical study is performed. Moreover, a sensitivity analysis allows us to implement an optimal strategy for the unknown parameter identification. Forward model and inverse problem are validated both on numerical simulation and known materials. Then, the presented experimental device developed is implemented for the analysis of orthotropic materials.

Nomenclature

Latin letters

Bi	Biot number
C_p	constant pressure specific heat (J kg^{-1} K^{-1})
M	modulus of the periodic component T_{periodic} (K)
R	radius of the heat flux distribution (m)
T	temperature (K)
T_{steady}	steady component of the temperature T (K)
T_{periodic}	periodic component of the temperature T (K)
X^*	reduced sensitivity functions
e	thickness (m)

f	frequency (Hz)
h	convective heat transfer coefficient (W m^{-2} K^{-1})
t	time (s)
(x, y, z)	space coordinate (m)
z	axial coordinate (m)

Greek letters

Φ	heat flux (W m^{-2})
α	thermal diffusivity (m^2 s^{-1})
β	model parameters
φ	phase lag (rad)
η	observable
λ	thermal conductivity (W m^{-1} K^{-1})
μ	diffusion length (m)
ρ	density (kg m^{-3})
ω	time pulsation (rad s^{-1})
(ω_x, ω_y)	spatial Fourier pulsations
$\tau(\omega_x, \omega_y, z, \omega)$	complex Fourier transform of the temperature
$\Theta(\omega_x, \omega_y)$	complex amplitude of the heat flux 2D spatial Fourier transform

1. Introduction

The development of new materials in order to obtain attractive properties in usual terms is a crucial step for industrial purposes. Material processing improvement as well as specific property achievement often requires a relevant predictive model and thus an accurate material properties identification. Thermal properties measurement is a crucial problem that affects many areas of engineering and material science. Many well-known identification methodologies are based on the observation of a material's thermal behaviour exposed to a calibrated excitation. These dynamic methods are usually classified according to the type of thermal excitation, the more usual being the step function, the Dirac pulse, the sine-wave modulation and more recently the pseudo-random sequences. Each of these categories of methods includes advantages and drawbacks that means either can be more applicable in a given configuration.

Periodic methods enable us to deduce thermal properties of a material from observations of its behaviour when it is submitted to a periodic heat source. The main advantage of these methods is to allow the periodic signal repetition many times. Thus, they can be used when the signal-to-noise ratio on observable output is low. The periodic excitation is generally made out on a limited volume whose characteristic dimension depends on diffusion properties of the sample and on the excitation frequency (see, for example, Autrique *et al* (2007 for an application to microscale thermal investigations).

In the following, a complete methodology dedicated to thermal characterization using a non-invasive periodic optical technique is proposed. Based on infrared observations, the presented measurement technique is attractive for global estimation in heterogeneous materials when other non-invasive optical techniques are usually devoted to local behaviour analysis. Its main advantage when compared with forced Rayleigh light scattering or pulsed photothermal radiometry is to provide observations over a geometrical domain which can be adapted to the studied material and to the thermal phenomena scale. For example, investigations can be performed on orthotropic materials in a real three-dimensional model, which takes

into account the spatial heterogeneity of the studied material (carbonic fibres in an epoxy matrix, for example). However, pulsed photothermal radiometry is best suited for thin film samples characterization (Macedo *et al* 2008), while forced Rayleigh light scattering can be implemented in a wide range of materials (organic liquids, ruby crystals, ...); see (Venerus *et al* 1999) for an application of this technique to thermal diffusivity estimation.

In order to widely investigate the proposed approach, modelling of thermal waves in the frequency domain, direct problem resolution, sensitivity analysis, data inversion, experimental device and experimental results are successively addressed.

In the following section, the heat transfers modelling in a domain submitted to a surface periodic heating input is investigated. Relevant observations for analysis in the frequency domain are usually both the modulus and phase lag of the output signal. A forward system based on partial differential equations is shown and forward problem is solved thanks to an inverse Fourier transform. Then, results of sensitivity analysis are discussed. In this section, the aim is to propose an optimal methodology: nuisance parameters are carefully investigated in order to minimize their effects on the relevant observable. Thermal diffusivity can be estimated thanks to observations either versus the excitation frequency or versus the distance from the excitation. In the specific case of anisotropic materials characterization, while a frequency sweep at a single space point cannot be used, it is shown that the use of a space distribution of the observable on the rear face (state for a single time frequency) ensures planar thermal diffusivities identification. The algorithms implemented for both the forward and the inverse problem resolutions are validated for numerical situations described in section 4. Experimental device which has been developed for materials characterization is then exposed. In section 6, several applications are proposed: the first one is dedicated to known metallic samples for validation purposes, while an unknown orthotropic material is studied for the second one.

2. The general principle of periodic methods and modelling in the frequency domain

The basic principle of these methods, devised by Angström (1863), is to periodically heat a sample and to measure the temperature along the sample which varies with the same period but with diminishing amplitude. Moreover, as the temperature wave travels along the sample with finite velocity there is a varying phase relationship. Measurement of the amplitude decrement and either the phase difference or velocity enables the diffusivity to be determined. As with static methods it is necessary to use a solution of the considered problem, which is appropriate to a particular experimental arrangement and to the boundary conditions. Periodic excitation signals can be and usually are designed to excite only a frequency band of interest and they have no significant power outside that band. This helps to keep excitation power as low as possible and to avoid on one hand unnecessary nonlinear effects, and on the other hand material damages.

Temperature measurements can be performed in two kinds of configuration for plane samples (figure 1):

- the first one (reflection) where temperature measurement and excitation are realized on the same sample side;
- the second one (transmission) where temperature measurement and excitation are realized on the opposite face of the sample.

Evolution of the system state (temperature T) at instant t for each point $(x, y, z) \in \mathbb{R}^3$ of the sample periodically excited can be written as a sum of two components:

$$T(x, y, z; t) = T_{\text{transient}}(x, y, z; t) + T_{\text{oscillating}}(x, y, z; t), \tag{1}$$

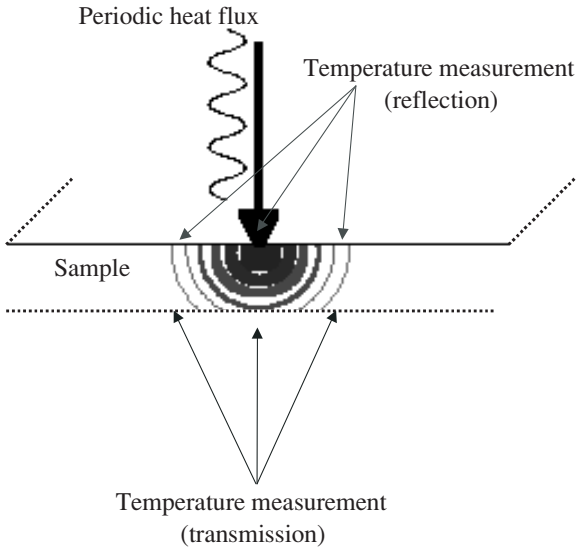

Figure 1. Temperature measurement configurations.

where $T_{\text{transient}}(x, y, z; t)$ is an increasing function of t (see figure 2) and $T_{\text{transient}}(x, y, z; t) \xrightarrow[t\to\infty]{} T_{\text{steady}}(x, y, z)$. In experimental configurations, system observations are performed once the transient component ceases: for $t \geqslant t_{\text{steady}}$. Various techniques can be implemented in order to estimate t_{steady} and in practice, the noise level has to be taken into account. For the specific framework related to the applications (materials thermal diffusivity identification) presented in section 6, authors consider that the steady state is reached if during 20 periods, both the maximum temperature and the minimum temperature for each period i $\left(T_i^{\max}, T_i^{\min}\right)$ satisfy for $i = 1, \ldots, 20$: $\tilde{T}^{\max} - \delta < T_i^{\max} < \tilde{T}^{\max} + \delta$ and $\tilde{T}^{\min} - \delta < T_i^{\min} < \tilde{T}^{\min} + \delta$, where $\tilde{T}$ is the average value of T_i (considering 20 periods) and δ depends on the standard deviation of the temperature measurements.

For $t \geqslant t_{\text{steady}}$, considering that the steady state is reached, the sample temperature can be written as a sum of a steady component and a periodic component whose period is the same as excitation (Gurevich *et al* 2003, Muscio *et al* 2004).

$$T(x, y, z; t) = T_{\text{transient}}(x, y, z, t) + T_{\text{oscillating}}(x, y, z; t) \xrightarrow[t\to\infty]{} T_{\text{steady}}(x, y, z) + T_{\text{periodic}}(x, y, z; t),$$

with $T_{\text{periodic}}(x, y, z; t)$ being a periodic non-harmonic signal written as (2) for a given angular frequency ω (rad s^{-1}):

$$T_{\text{periodic}}(x, y, z; t) = \sum_{k=1}^{\infty} M_k(x, y, z)\, \mathrm{e}^{\mathrm{j}k\omega t}\, \mathrm{e}^{\mathrm{j}\varphi_k(x,y,z)}, \tag{2}$$

where M_k (K) is the modulus and φ_k (rad) is the phase lag of the kth harmonic. M_k and φ_k depend also on ω.

Both modulus M_k and phase lag φ_k are connected to thermal properties of the material. (Note that for an orthotropic material, the thermal conductivities tensor is diagonal). Thus,

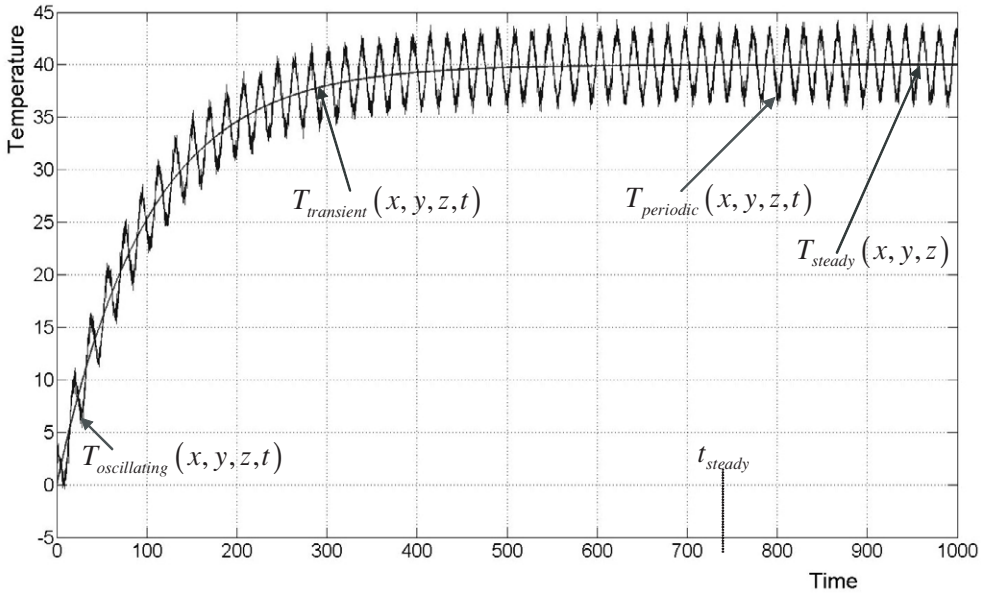

Figure 2. Phase lag and modulus definition.

considering ρ to be the density (kg m^{-3}), C_p the specific heat (J kg^{-1} K^{-1}), and

$$\vec{\vec{\lambda}} = \begin{bmatrix} \lambda_x & 0 & 0 \\ 0 & \lambda_y & 0 \\ 0 & 0 & \lambda_z \end{bmatrix}$$

the thermal conductivities tensor (W m^{-1} K^{-1}), it comes

$$\vec{\vec{\alpha}} = \begin{bmatrix} \alpha_x & 0 & 0 \\ 0 & \alpha_y & 0 \\ 0 & 0 & \alpha_z \end{bmatrix}$$

the thermal diffusivities tensor where $\alpha_i = \frac{\lambda_i}{\rho C_p}$ en (m^2 s^{-1}). $\mu = \sqrt{\frac{\max \vec{\vec{\alpha}}}{\pi f}}$ is called diffusion length (the excitation frequency is denoted by f (Hz)). It is usual to consider that at a distance up to 3μ, at least 95% of the thermal wave has disappeared.

In this work, we want to identify:

- the thermal diffusivity of isotropic materials (the thermal conductivities tensor is a constant) from phase-lag observations in any point;
- the thermal diffusivities tensor of orthotropic materials from phase-lag observations versus the three main axes.

The considered problem and its simplified geometry are shown in figure 3.

Let us consider an e thick versus z-axis orthotropic material, where the x and y dimensions are chosen so that boundary effects are neglected on the lateral faces of the plane-parallel sample. The thermal excitation produced by a periodic heat flux is centred on its front face in $(x, y, z) = (0, 0, 0)$. The convective heat losses h (W m^{-2} K^{-1}) are taken into account on the

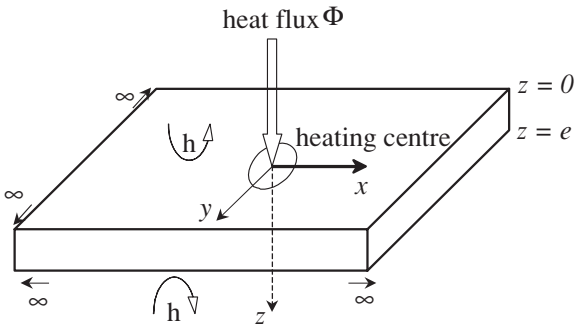

Figure 3. Simplified geometry of the forward model.

front face ($z = 0$) and on the back face ($z = e$) of the sample. The system state evolution is described by the following heat equation:

$$\rho C_p \frac{\partial T}{\partial t} = \operatorname{div}(\vec{\lambda}\,\overrightarrow{\operatorname{grad} T}). \tag{3}$$

Boundary conditions are

$$\begin{cases} z = 0: & -\lambda_z \dfrac{\partial T(x, y, 0, t)}{\partial z} = \Phi(x, y, 0, t) - hT(x, y, 0, t) \\ z = e: & -\lambda_z \dfrac{\partial T(x, y, e, t)}{\partial z} = hT(x, y, e, t), \end{cases} \tag{4}$$

where $\Phi(x, y, 0; t)$ is the periodic heat flux in (W m^{-2}). Without lack of generality, initial condition in the whole domain is written such as:

$$t = 0: \qquad T = 0. \tag{5}$$

In most non-academic situations, the forward model (3)–(5) is quite difficult to solve by an analytical way in the real space. Moreover, numerical resolution is not appropriate since time evolution analysis is less relevant than modulus and the phase-lag analysis (in steady state). Thus, a complex Fourier transform versus x and y axes can be implemented. Let $\tau(\omega_x, \omega_y, z, \omega)$ be this complex Fourier transform:

$$\tau(\omega_x, \omega_y, z, \omega) = \int_{\mathbb{R}^2} M_1(x, y, z, \omega)\, \mathrm{e}^{-\mathrm{j}\omega_x x}\, \mathrm{e}^{-\mathrm{j}\omega_y y}\, \mathrm{e}^{\mathrm{j}\varphi_1(x,y,z,\omega)}\, \mathrm{d}x\, \mathrm{d}y, \tag{6}$$

where ω_x and ω_y are the spatial Fourier pulsations. Let us assume that flux excitation has a 'top hat' space distribution of radius R, and a periodic time evolution with angular pulsation $\omega = 2\pi f$. The corresponding 2D Fourier transform $\Theta(\omega_x, \omega_y)$ can be written such as:

$$\Theta(\omega_x, \omega_y) = \int_{\mathbb{R}^2} \Phi(x, y) \cos(\omega_x x) \cos(\omega_y y)\, \mathrm{d}x\, \mathrm{d}y = \frac{2\pi \Phi_0 R J_1\left(R\sqrt{\omega_x^2 + \omega_y^2}\right)}{\sqrt{\omega_x^2 + \omega_y^2}} \tag{7}$$

with R (m) being the heat source radius and J_1 the Bessel function of the first kind. In fact, periodic excitation signals have been chosen in order to excite only a frequency band of interest. So they have no significant power outside the first harmonic. Thus, considering $\tau(\omega_x, \omega_y, z, \omega)$ in (3) and by dividing (3) by ρC_p it comes

$$\left(-\omega_x^2 \alpha_x - \omega_y^2 \alpha_y - \mathrm{j}\omega\right)\tau(\cdot) + \alpha_z \frac{\partial^2 \tau(\cdot)}{\partial z^2} = 0. \tag{8}$$

Equation (4) becomes

$$\begin{cases} z = 0: & -\lambda_z \dfrac{\partial \tau}{\partial z} = \Theta - h\tau, \\ z = e: & -\lambda_z \dfrac{\partial \tau}{\partial z} = h\tau. \end{cases} \tag{9}$$

It is important to note that $\tau(\cdot)$ is not time dependent and solution of system (8), (9) is as follows:

$$\tau(\cdot) = \left[\frac{(\lambda_z r + h)\Theta(\cdot)}{(\lambda_z r + h)^2 + (\lambda_z r - h)^2 \exp^{-2er}}\right] \exp^{-rz} + \left[\frac{(\lambda_z r - h)\exp^{-2er}\,\Theta(\cdot)}{(\lambda_z r + h)^2 + (\lambda_z r - h)^2 \exp^{-2er}}\right] \exp^{+rz}, \tag{10}$$

with $r = \sqrt{\frac{\omega_x^2 \alpha_x + \omega_y^2 \alpha_y + \mathrm{j}\omega}{\alpha_z}}$. At this step, it can be possible to put in evidence the Biot number: $Bi = \frac{he}{\lambda_z}$ in equation (10) such as:

$$\tau(\cdot) = \left[\frac{(er + \mathrm{Bi})\Theta(\cdot)e}{\lambda_z((er + \mathrm{Bi})^2 - (er - \mathrm{Bi})^2 \exp^{-2er})}\right] \exp^{-rz} + \left[\frac{(er - Bi)\,\mathrm{e}^{-2er}\Theta(\cdot)e}{\lambda_z((er + Bi)^2 - (er - Bi)^2 \exp^{-2er})}\right] \exp^{+rz}. \tag{11}$$

Then, for a known set of input parameters $\{\alpha_i, \lambda_z, Bi, R, \omega, e, \Phi_0\}$, the complex Fourier transform of the temperature $\tau(\omega_x, \omega_y, z, \omega)$ is obtained thanks to the computation of the spatial Fourier pulsations (ω_x, ω_y). The return in temperature space is obtained by means of an inverse Fourier transform defined by

$$M_1(x, y, z, \omega)\,\mathrm{e}^{\mathrm{j}\varphi_1(x,y,z,\omega)} = \iint_{\mathbb{R}^2} \tau(\omega_x, \omega_y, z, \omega)\,\mathrm{e}^{\mathrm{j}\omega_x x}\,\mathrm{e}^{\mathrm{j}\omega_y y}\,\mathrm{d}\omega_x\,\mathrm{d}\omega_y. \tag{12}$$

Then, calculation of the inverse Fourier transform is numerically performed to determine both phase lag φ_1 and modulus M_1. For the numerical implementation, it is important to note that the studied geometry is such that the material is assumed to be a semi-infinite plate (see figure 3). For experimental configurations, it is quite important to verify that lateral boundaries effects do not affect thermal waves propagation: sample dimensions among x and y axes have to be large enough (greater than 3μ). Then equation (12) is numerically solved:

$$M_1(x, y, z, \omega)\,\mathrm{e}^{\mathrm{j}\varphi_1(x,y,z,\omega)} = \int_{\Omega_F \subset \mathbb{R}^2} \tau(\omega_x, \omega_y, z, \omega)\,\mathrm{e}^{\mathrm{j}\omega_x x}\,\mathrm{e}^{\mathrm{j}\omega_y y}\,\mathrm{d}\omega_x\,\mathrm{d}\omega_y,$$

where $\Omega_F = \left[-\omega_x^{\max}, \omega_x^{\max}\right] \times \left[-\omega_y^{\max}, \omega_y^{\max}\right]$ is defined such that signal energy is closed to zero in $\mathbb{R}^2 - \Omega_F$. For $(x, y) \in \mathbb{R}^2 - \Omega_F$, $M_1(x, y, z, \omega)\,\mathrm{e}^{\mathrm{j}\varphi_1(x,y,z,\omega)} \approx 0$. Both $\omega_x^{\max}$ and $\omega_y^{\max}$ are numerically obtained considering the energy spectral density. Then,

$$M_1(x, y, z, \omega)\,\mathrm{e}^{\mathrm{j}\varphi_1(x,y,z,\omega)} = \int\limits_{\Omega_F \subset \mathbb{R}^2} f(\cdot)\,\mathrm{d}\omega_x\,\mathrm{d}\omega_y = \sum\nolimits_{k/P_k \subset \Omega_F} \tilde{f}_k A_k$$

where P_k is the kth rectangular element of the discretized domain Ω_F, P_k surface is denoted by A_k and $\tilde{f}_k = \underset{P_k}{\mathrm{mean}}(\tau(\omega_x, \omega_y, z, \omega)\,\mathrm{e}^{\mathrm{j}\omega_x x}\,\mathrm{e}^{\mathrm{j}\omega_y y})$. Angular space frequency discretization (determining P_k) is chosen such that $M_1(x, y, z, \omega)\,\mathrm{e}^{\mathrm{j}\varphi_1(x,y,z,\omega)}$ computation is not affected by a more accurate discretization.

In figure 4, an example of numerical results is shown for an orthotropic material according to the following data: $\alpha_x = 3.7 \times 10^{-6}$ m^2 s^{-1}, $\alpha_y = \alpha_z = 4.5 \times 10^{-7}$ m^2 s^{-1}, $\lambda_z = 0.7$ W m^{-1} K^{-1}, $Bi = 0.07$, $R = 2 \times 10^{-3}$ m, $\omega = 0.005$ rad s^{-1} and $e = 5 \times 10^{-3}$ m. Modulus is expressed as the dimensionless ratio: $\bar{M} = \frac{M(x,y,z)}{\max M(x,y,z)} = \frac{M(x,y,z)}{M(0,0,0)}$.

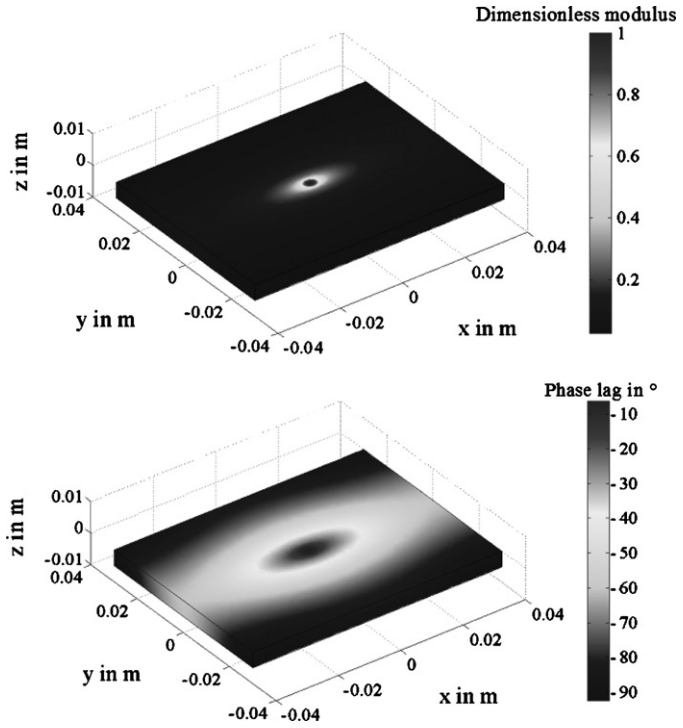

Figure 4. Phase lag and modulus estimated for an orthotropic material.

The ellipsoidal shape of both modulus and phase-lag distributions is characteristic of orthotropic material ($\alpha_x \neq \alpha_y$) thermal behaviour when submitted to a periodic excitation. In the following section, a brief sensitivity analysis is performed in order to investigate the interest of phase-lag observation in order to identify thermal diffusivity.

3. Sensitivity analysis

In order to optimize the identification methodology, sensitivity analysis is a crucial requirement and several key points have to be investigated:

- Are modulus and phase-lag observations able to estimate thermal diffusivity?
- Several model parameters are assumed to be known. It is essential to determine if their uncertainties do no dramatically affect the thermal diffusivity identification.
- Some ambient parameters are quite difficult to control and their effects have to be as weak as possible. From the experimental point of view, it is obvious for example that the convective exchange coefficient is a nuisance parameter.

While the process state evolution is obtained by considering resolution of a set of partial differential equations $\{S_{\text{dir}}\}$ (and solving a forward problem), the sensitivity analysis is performed by computing the sensitivity functions which are solutions of the sensitivity problem derived from $\{S_{\text{dir}}\}$. A sensitivity study of an observable η (in our case, the observed phase lag or the modulus of the measured temperature $\eta = \{M, \varphi\}$) on model parameters $\beta = \{\alpha_i, \lambda_z, Bi, R, \omega, e, \Phi_0\}$ allows either to reduce the forward model or to discuss the

possibility of accurate physical parameters identification (Beck and Arnold 1977). Sensitivity functions are defined as the absolute variation of the observable induced by an absolute variation of the considered parameter. In order to compare these coefficients with each other, the reduced sensitivity functions of η_i versus parameter β_j are defined by the following relation:

$$X^*_{\eta_i,\beta_j} = \beta_j \frac{\partial \eta_i(\beta)}{\partial \beta_j}. \tag{13}$$

It is important to note that this reduced sensitivity function represents not only the amplitude variation but also its sign. For a given application, if the reduced sensitivity function versus an unknown parameter is weak on the considered domain (space, time, frequency domain ...) then information on this parameter contained in observable measurements is poor. It comes that if this reduced function is equal to zero, then the considered parameter cannot be identified from this observable. Moreover, if the reduced functions versus two parameters are linearly dependant, it can only be possible to identify a relationship between these two parameters. This sensitivity study has to be performed for the unknown parameters but also for the known parameters (which are *a priori* known with given uncertainties). It is usual to reduce the number of uncertain parameters in order to simplify the sensitivity analysis. However, in a preliminary step, a screening procedure based on numerical design of experiment can be implemented in order to determine which reduced sensitivity functions $X^*_{\eta_i,\beta_j}$ have to be carefully investigated (see Rouquette *et al* 2007).

Usually, a design of experiment (DOE) is a set of experimental runs that are chosen in order to estimate the factor effect on a response; see, for example, Montgomery (1997). In a numerical situation, considering a model describing the relation between a desired property and some process parameters, a set of numerical runs is analysed and model analyses are proposed.

In a second step, the choice of the non-studied parameters can be based upon *a priori* knowledge, experimental results, etc. Three methods have usually been used to calculate these reduced sensitivity functions:

- if an analytical solution of the forward problem exists, directly by calculating the corresponding derivative;
- if the forward problem is nonlinear versus parameters, by calculating the Gateau derivative; see for example an application in Abou Khachfe and Jarny (2001);
- if only a numerical or a semi-analytical solution of the forward problem exists, by calculating the corresponding numerical derivative.

Then, it becomes evident that the sensitivity study must be carefully performed in order to determine parameter identifiability. In the following, the interest of periodic approach in several configurations is stated.

3.1. Example of sensitivity analysis for a steel sample: frequency scanning

Let us consider the specific geometry described in figure 3 where the sample is a steel thin plate. We are mainly interested in the identification of its thermal conductivity λ while ρC_p is assumed to be known. Then, the model parameters are $\beta = \{\rho C_p, \lambda, Bi, R, \omega, e, \Phi_0\}$. Let us consider the following parameters: $\rho C_p = 3.7 \times 10^6$ J K^{-1} m^{-3}, $e = R = 2 \times 10^{-3}$ m and $Bi = 4.6 \times 10^{-4}$. For sensitivity analysis, a value has to be chosen for the unknown parameter and let us assume that $\lambda = 40$ W m^{-1} K^{-1}. In this example (in transmission), thermal behaviour of the steel sample is observed in the centre of the non-solicited face while a frequency range is scanning $\frac{\omega}{2\pi} = f \in [0.01, 1]$.

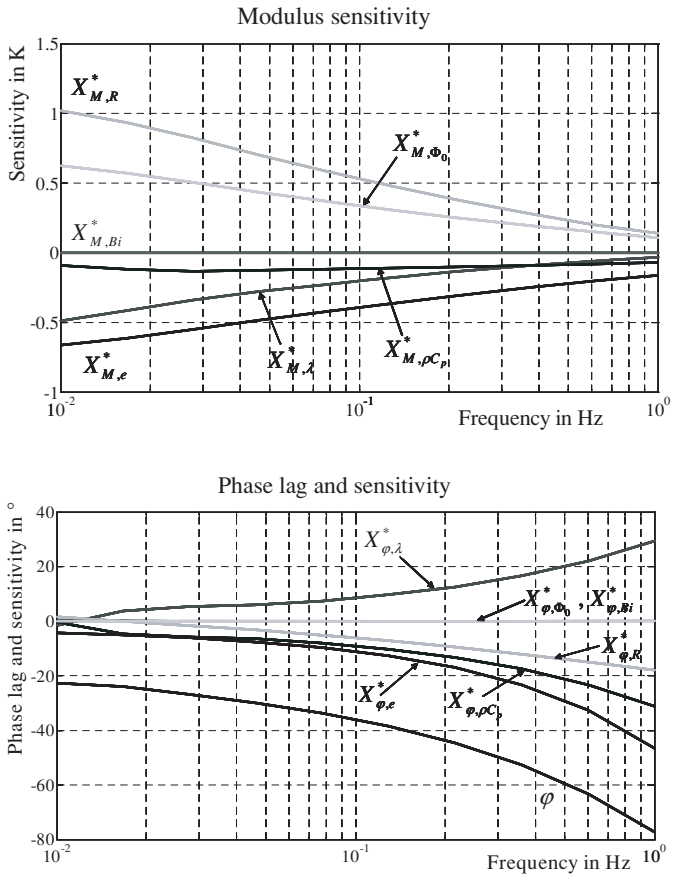

Figure 5. Reduced sensitivity functions for a frequency scanning (example of a steel plate).

Reduced sensitivity functions are estimated by discretizing these partial derivatives. Results are shown in figure 5 for both modulus and phase lag. It is obvious that thermal conductivity λ cannot be estimated using modulus measurements. In fact, since $\left|X^*_{M,\Phi_0}\right| > \left|X^*_{M,\lambda}\right|$, parameters characterizing heating flux (which are quite difficult to quantify) are considered as nuisance parameters which prevent from estimating λ considering M observations. In the following, only phase-lag measurements are taken into account. It is shown in figure 5 that for thermal conductivity identification, it is essential to accurately known $\{\rho C_p, R, e\}$ while phase lag does not depend on $\{Bi, \Phi_0\}$. It is important to note that this methodology is dedicated to thermal diffusivity $\alpha = \frac{\lambda}{\rho C_p}$ identification and then it is obvious that λ identification is meaningful if ρC_p is well known. Lastly, if modulus is great enough to ensure signal observations, experiments can be performed for high frequency.

3.2. Example of sensitivity analysis for an insulating material: spatial scanning

In this studied situation (in transmission), thermal behaviour of the sample is observed along the x-axis for a given frequency. Let us consider a glass thin plate. Model parameters are $\beta = \{\alpha, \lambda, Bi, R, \omega, e, \Phi_0\}$. Let us consider the following parameters: $\lambda \approx 1.4$ W m^{-1} K^{-1},

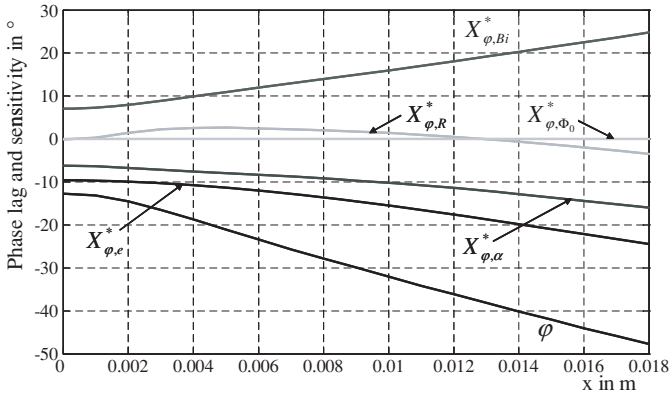

Figure 6. Reduced sensitivity functions for a spatial scanning (example of a glass plate, $f = 0.001$ Hz).

$\rho C_p \approx 1.5 \times 10^6$ J K^{-1} m^{-3}, $\alpha \approx \frac{1.4}{1.5\times10^6} \approx 0.9 \times 10^{-6}$ m^2 s^{-1}, $e = R = 2 \times 10^{-3}$ m and $Bi = 1.4 \times 10^{-2}$. Thermal conductivity (that is λ_z in equations (9) and (11)) is taken into account in Biot number definition. Thus $|X^*_{\varphi,\lambda}|$ is not considered but only $|X^*_{\varphi,\alpha}|$ and $|X^*_{\varphi,Bi}|$ are investigated in this paragraph. For a given frequency, $f = 0.001$ Hz, it is shown in figure 6 that

- heating flux amplitude (Φ_0) inaccuracies have no influence on phase lag;
- $|X^*_{\varphi,e}| > |X^*_{\varphi,\alpha}|$: sample thickness ($e$) has to be accurately known;
- $|X^*_{\varphi,Bi}| > |X^*_{\varphi,\alpha}|$: thus, for low frequency, since convective exchange is quite difficult to estimate, thermal diffusivity identification cannot be performed.

For a greater given frequency, $f = 0.01$ Hz, thermal diffusion length is $\sqrt{10}$ times lower. Then, thermal transfers are quite different as is shown in figure 7. Thus, for high frequency, it is shown that if the heating source spatial distribution radius (R) has to be accurately known, a specific spatial range (for this example $x \in [0, 0.015]$) can be considered for phase-lag observations. In fact, in this spatial range and at this given frequency, $|X^*_{\varphi,Bi}| \ll |X^*_{\varphi,\alpha}|$. Then, inaccuracies on convective exchange estimation do not dramatically affect thermal diffusivity identification.

3.3. Example of sensitivity analysis for an orthotropic material

Let us considered the orthotropic material studied in section 2: $\alpha_x = 3.7 \times 10^{-6}$ m^2 s^{-1}, $\alpha_y = \alpha_z = 4.5 \times 10^{-7}$ m^2 s^{-1}, $\lambda_z = 0.7$ W m^{-1} K^{-1}, $Bi = 0.07$, $R = 2 \times 10^{-3}$ m and $e = 5 \times 10^{-3}$ m. Two configurations can be considered in transmission: thermal behaviour of the sample observed in the centre of the non-solicited face while a frequency range is scanning (case 1) or among each axis (in the plane $(0, x, y)$) for a given frequency (case 2). Phase-lag sensitivity to heating flux (Φ_0) amplitude is neglected since it has been shown equal to zero in sections 3.1 and 3.2.

Case 1: frequency scanning $\frac{\omega}{2\pi} = f \in [0.001, 0.1]$
In figure 8, it is shown that thermal diffusivity identification among z-axes (α_z) can be performed considering phase-lag measurements in the centre of the non-solicited face while $f \in [0.001, 0.1]$ if the material thickness is known with a great accuracy. It

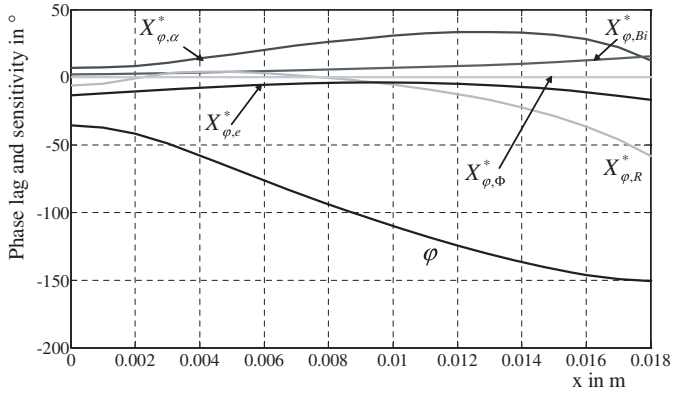

Figure 7. Reduced sensitivity functions for a spatial scanning (example of a glass plate, $f = 0.01$ Hz).

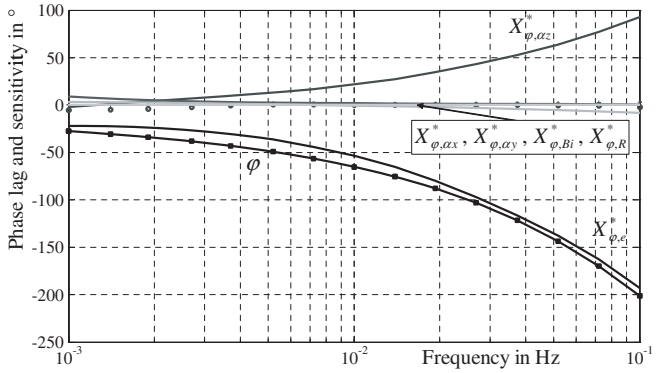

Figure 8. Reduced sensitivity functions for a frequency scanning (example of an orthotropic material).

is important to note that inaccuracies in (α_x, α_y) do not affect the (α_z) estimation since $\left|X^*_{\varphi,\alpha_x}\right| \approx \left|X^*_{\varphi,\alpha_y}\right| \ll \left|X^*_{\varphi,\alpha_z}\right|$.

Case 2: spatial scanning versus Ox and Oy: $(x, y) \in [0, 0.015]^2$
In figure 9, it is shown that if the material thickness is known, thermal diffusivity identification among x-axes (α_x) can be performed considering phase-lag measurements among x-axes:

- for $x < 0.005$ if (α_z) is well known (thanks to a preliminary frequency scanning as in case 1) since $\left|X^*_{\varphi,\alpha_x}\right| \gg \left|X^*_{\varphi,\alpha_y}\right| \approx \left|X^*_{\varphi,R}\right| \approx \left|X^*_{\varphi,Bi}\right|$;
- for $x > 0.01$ since $\left|X^*_{\varphi,\alpha_x}\right| \gg \left|X^*_{\varphi,\alpha_z}\right| \approx \left|X^*_{\varphi,\alpha_y}\right| \approx \left|X^*_{\varphi,R}\right| \approx \left|X^*_{\varphi,\mathrm{Bi}}\right|$.

In figure 10, it is shown that the material thickness has always to be well known and several areas can be considered for the identification of the thermal diffusivity identification among y-axes (α_y) considering phase-lag measurements among y-axes

- for $x < 0.005$ if (α_z) is well known (thanks to a preliminary frequency scanning as in case 1) since $\left|X^*_{\varphi,\alpha_y}\right| \gg \left|X^*_{\varphi,\alpha_x}\right| \approx \left|X^*_{\varphi,R}\right| \approx \left|X^*_{\varphi,Bi}\right|$;
- for $x > 0.005$, the heating source spatial distribution radius (R) has to be accurately known and $\left|X^*_{\varphi,\alpha_y}\right| \gg \left|X^*_{\varphi,\alpha_z}\right| \approx \left|X^*_{\varphi,\alpha_x}\right| \approx \left|X^*_{\varphi,Bi}\right|$.

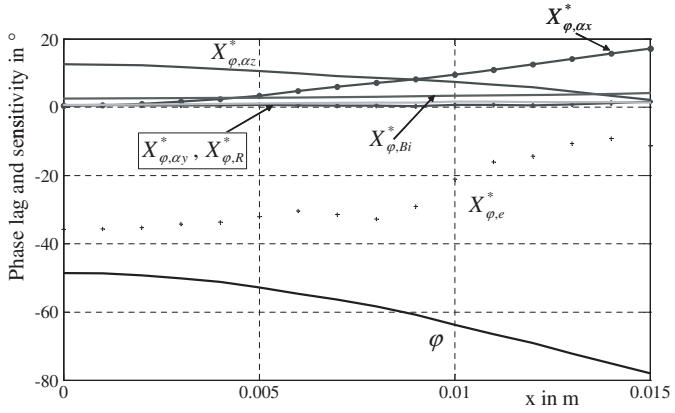

Figure 9. Reduced sensitivity functions for a spatial scanning versus x (example of an orthotropic material $f = 0.005$ Hz).

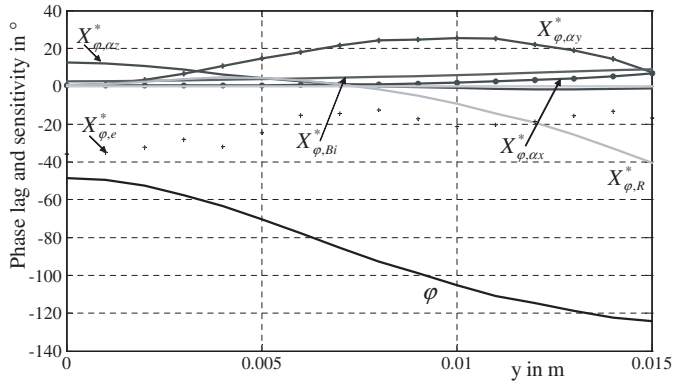

Figure 10. Reduced sensitivity functions for a spatial scanning versus y (example of an orthotropic material $f = 0.005$ Hz).

Let us note that even if $|X^*_{\varphi,e}|$ is obtained with numerical noises, the trend is verified and it is crucial to accurately know the material thickness.

4. Thermal diffusivity identification considering noisy disturbed simulated phase lag

Previous sensitivity analysis has shown the interest of the methodology based upon periodic solicitations and phase-lag observations for thermal diffusivity identification. In the following, a minimization algorithm is presented and results are discussed. A Levenberg–Marquardt numerical algorithm (Levenberg 1944, Marquardt 1963) for the resolution of the inverse problem has been developed in order to identify the unknown parameter α considering given parameters $\{Bi, R, \omega, e\}$ and phase-lag observations (Alifanov 1994, Isakov 1998, Walter and Pronzato 1997).

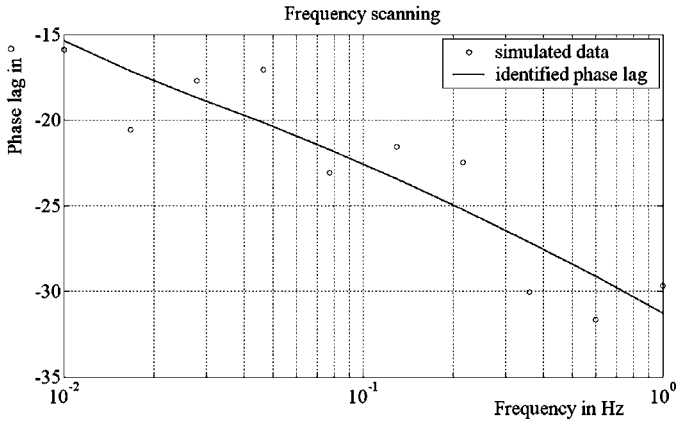

Figure 11. Example of simulated phase lags and estimated phase lag for frequency scanning.

The Levenberg–Marquardt algorithm provides a numerical solution to the problem of minimizing a quadratic criterion $\chi^2(\alpha)$ describing the difference between measured phase lags $\hat{\varphi}_i$ and simulated phase lags φ_i:

$$\chi^2(\alpha) = \sum (\hat{\varphi}_i - \varphi_i(\alpha))^2. \tag{14}$$

The Levenberg–Marquardt algorithm is an iterative procedure and can be thought of as a combination of steepest descent and the Gauss–Newton method. In each iteration step, the parameter vector is modified and the corresponding function φ_i (issued from the forward problem resolution) is approximated by the computation of the Jacobian matrix of φ_i. Moreover, a damping term (Gill *et al* 1981) is adjusted at each iteration to assure a reduction in error.

Robustness of this approach is investigated while a realistic noise is generated on simulated data (a Gaussian random generator is used $N(0, 2)$). Noisy disturbed simulated phase lags are considered for both frequency scanning (in the centre of the non-irradiated face) and spatial scanning (at a given frequency). Let us consider a thermal conductor material and the following parameters: $Bi = 4.6 \times 10^{-4}$ and $e = R = 2 \times 10^{-3}$ m.

Case 1: frequency scanning
Sensitivity analysis has shown that thermal diffusivity α identification can be performed considering model parameters $\beta = \{Bi, R, \omega, e\}$. Let us consider the following frequency range: $\frac{\omega}{2\pi} = f \in [0.01, 1]$. Simulated phase lags are obtained for $\alpha = 10^{-5}$ m^2 s^{-1}. Identification results are presented in figure 11. Convergence is achieved in few iterations and identified thermal diffusivity is $\alpha = 9.7 \times 10^{-6}$ m^2 s^{-1}. Results are quite satisfactory since even noise is overestimated, convergence is fast and error on identified parameter is about 3%.

Case 2: spatial scanning
The given frequency is $f = 0.05$ Hz. Simulated phase lags are obtained for $\alpha = 10^{-5}$ m^2 s^{-1}. Identification results are presented in figure 12. Convergence is achieved in few iterations and identified thermal diffusivity is $\alpha = 9.9 \times 10^{-6}$ m^2 s^{-1}. Results are quite satisfactory since even noise is overestimated, convergence is fast and error on identified parameter is about 1%.

In figure 12, reduced sensitivity functions $X^*_{\varphi,\beta}$ with $\beta = \{Bi, R, \omega, e\}$ are plotted. Realistic uncertainties have been considered from the experimental point of view, since several nuisance parameters can be accurately measured independently. Let us consider: $Bi \pm 10\%$,

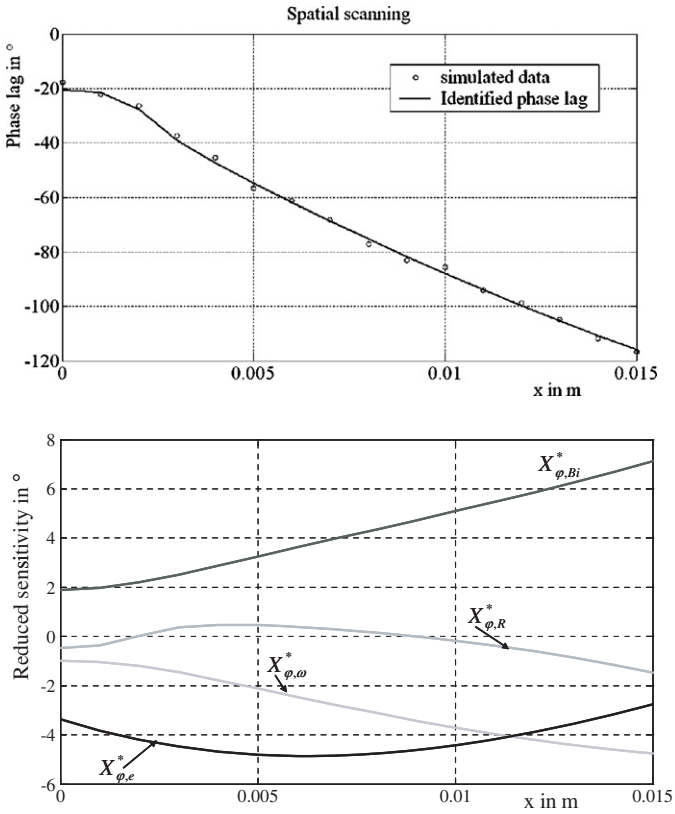

Figure 12. Example of reduced sensitivity, simulated phase lags and estimated phase lags for spatial scanning.

$R \pm 2\%$, $\omega \pm 1\%$ and $e \pm 2\%$. It is important to note that in a specific configuration, $|X^*_{\varphi,Bi}|$ can be reduced considering great excitation frequency (see section 3.2).

Thermal diffusivity identification has been performed according to several initial values of the minimization algorithm and results are quite accurate. Whatever the initial value is, and considering noisy disturbed simulated data, convergence of the minimization algorithm is achieved. Thus, the methodology seems to be relevant and the identification numerical algorithm is validated. An experimental device has been developed for identification based on our approach. Phase-lag measurements are performed by an infrared camera for two-dimensional analysis which is dedicated to orthotropic materials. For isotropic materials, a single axis scanning is sufficient and a cheaper pyrometer with an oscillating mirror can be implemented.

5. Measuring bench

An experimental device has been developed in order to identify thermal diffusivity of materials by non-destructive observations. This experimental bench comprises three main parts (see figure 13):

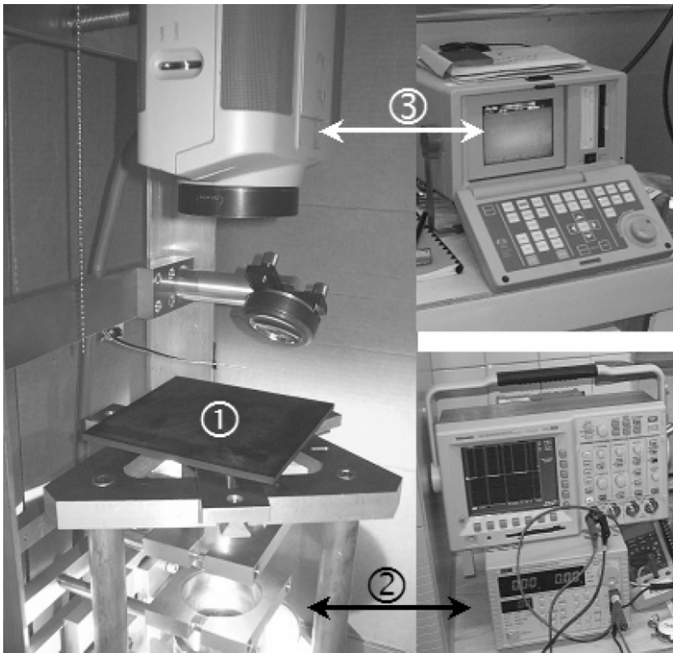

Figure 13. Experimental bench.

(1) The sample part where the tested material is located in the focal plane of a Köhler optical device.

(2) The excitation part constituted by a halogen lamp (36 V, 400 W) under this assembly associated with a process control to generate a periodic input (square, sinusoidal, ...) on the back face of the sample.

(3) The measurement part made up by an IR camera placed on the front face of the sample linked to a signal processing.

The spatial distribution of the temperature on the sample recorded by the IR camera is representative of the material's nature (isotropic for circular distribution, orthotropic for ellipsoidal distribution, ...). The signal processing allows extraction of the amplitude of the signal and the phase lag between periodic input and thermal response of the material, even if the noise level is high. Spatial distributions analysis is performed in order to define the sample geometry, the maximum temperature, the excitation frequency and the distance between IR camera and the observed face. 512 pictures are recorded in order to measure more than 10 periods.

A previous sensitivity analysis has shown that even if phase lag and modulus are measured, only phase-lag observations lead to a correct identification (since modulus is correlated to nuisance parameters). However, modulus cartographies are taken into account in order to determine the low level of attenuation for which output signal is not significant enough. Considering 512 pictures (256×100 pixels), modulus (corresponding to temperature amplitude around the steady state) and phase-lag cartographies are deduced thanks to a lock-in algorithm. Several experimentations have been performed in order to estimate the noise level for both the modulus (± 1 K) and the phase lag ($\pm 10\%$).

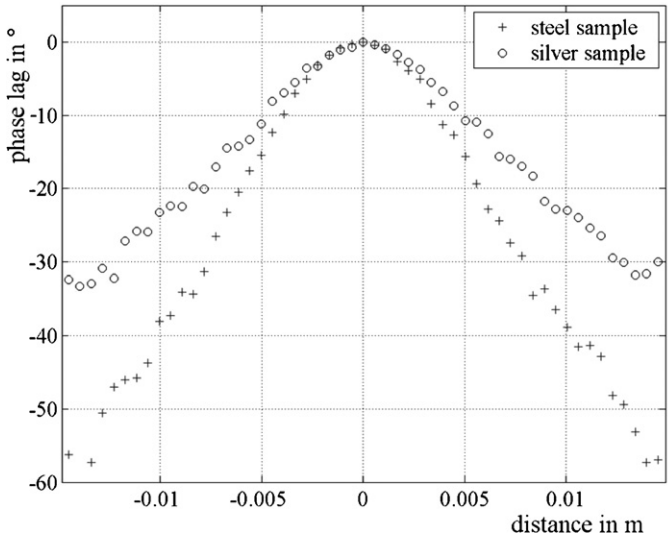

Figure 14. Phase-lag measurements.

6. Experimental results

In this section, the number of harmonics used to compute theoretical phase lag is $(nx)_{\max} = (ny)_{\max} = 512$.

6.1. Validation for isotropic materials

Experiments have been performed with known metallic materials in order to validate both the methodology and the experimental device. The heating source radius on the excited face is $R = 3 \times 10^{-3}$ m. The first sample is a steel thin plate ($e = 0.3 \times 10^{-3}$ m) exposed to an excitation frequency $f = 0.1$ Hz, while the second one is a silver thin sheet ($e = 0.1 \times 10^{-3}$ m; $f = 0.11$ Hz). Biot numbers are $Bi_{\text{steel}} = 3.7 \times 10^{-4}$ and $Bi_{\text{silver}} = 4.7 \times 10^{-6}$. Measured phase lags obtained thanks to the experimental device are shown in figure 14. Identification algorithm has been used for the inverse problem resolution. Then, identified thermal diffusivities are $\alpha_{\text{steel}} \approx 30 \times 10^{-6}$ m^2 s^{-1} and $\alpha_{\text{silver}} \approx 160 \times 10^{-6}$ m^2 s^{-1}. These values are much close to those of the literature (Brady *et al* 1997). Difference is less than 10%. The correct fit is shown in figure 15.

In the following section, identification results are presented for an unknown orthotropic material.

6.2. Test for orthotropic material

An orthotropic material (a fibre composite) has been studied. We are mainly interested in in-plane diffusivity identification (α_x and α_y) considering phase lag among x and y-axes observed for a fixed excitation frequency. In figure 16, a modulus distribution is shown for a given frequency.

The ellipsoidic shape is due to $\lambda_x \neq \lambda_y$. Heating power is chosen in order to avoid boundary effects (a semi-infinite plate has to be considered for the forward model). It is important to note that the spatial resolution of the infrared camera is different versus x-axis and

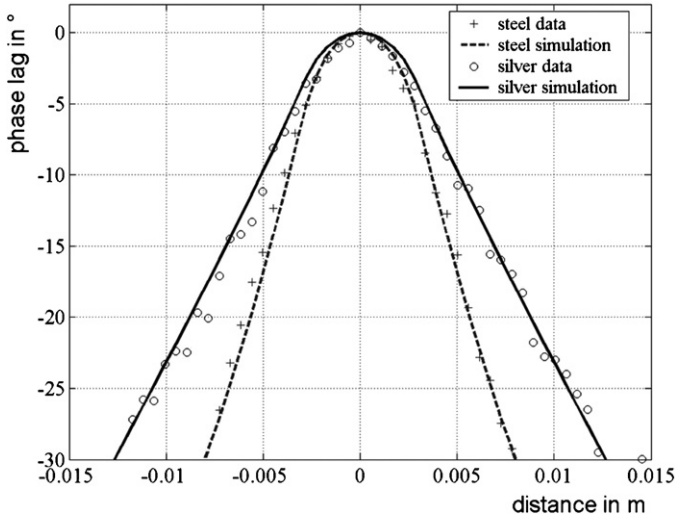

Figure 15. Measurements and simulation computed with identified values.

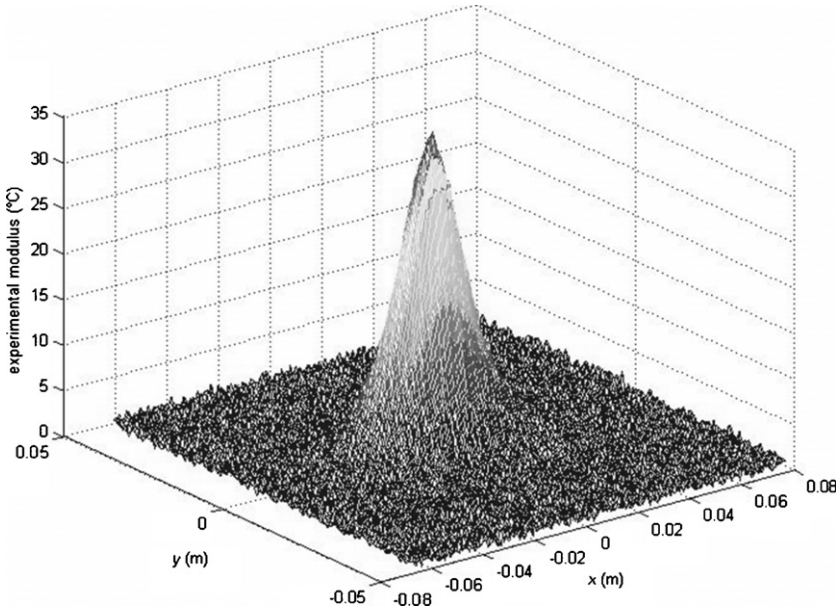

Figure 16. Modulus cartography for orthotropic material.

y-axis. Dimensions of rectangular pixels are $\Delta x \approx 0.56 \times 10^{-3}$ m and $\Delta y \approx 0.96 \times 10^{-3}$ m. Thus more accurate observations are obtained versus x-axis. Modulus (figure 16) can be considered to set the sample x-axis or y-axis. Relevant spatial domain is also deduced from figure 16 since modulus is also useful for the determination of the low level of attenuation for which output signal is not significant enough.

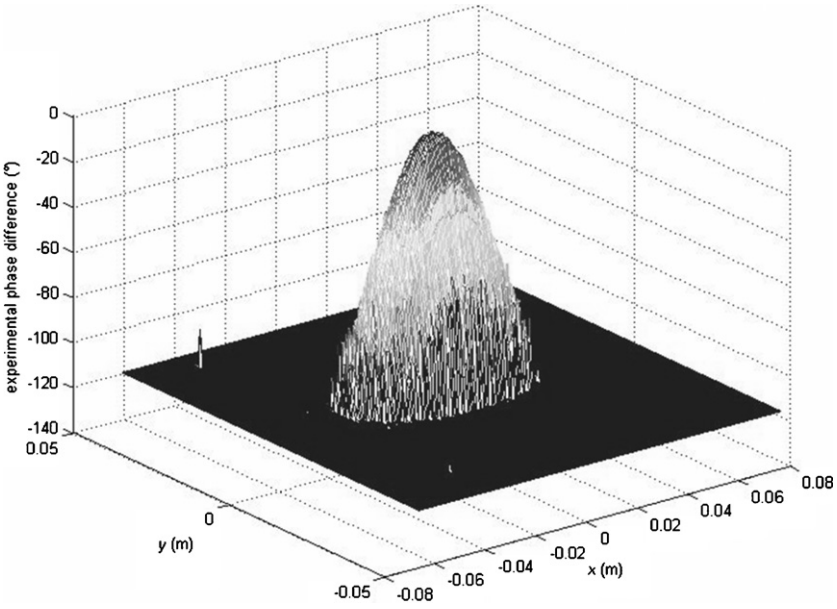

Figure 17. Phase-lag cartography for orthotropic material.

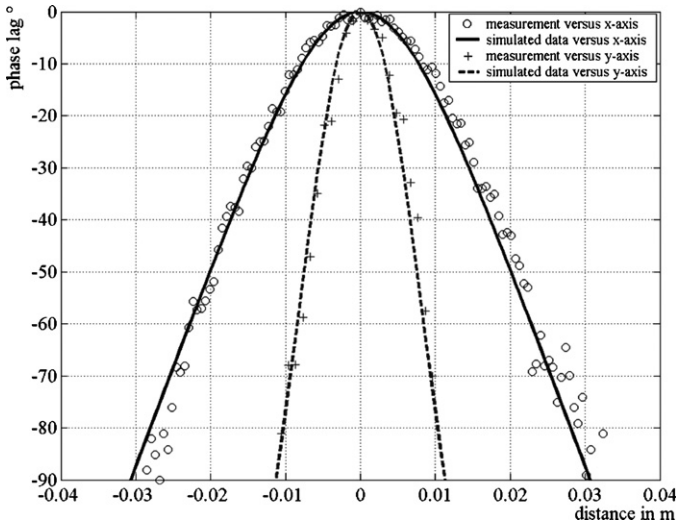

Figure 18. Identification results.

Then phase-lag cartography can be considered (see figure 17). The previous minimization algorithm has been modified to take into account the diffusivity tensor. Resolution has been performed according to the phase lag observed on each axis (deduced from cartography shown in figure 17).

The correct convergence of the algorithm is presented in figure 18 and it has been estimated that $\alpha_x \approx 10\alpha_y$ and that $\alpha_x \approx \alpha_z$. This preliminary result is characteristic of a fibre stack in a reinforced matrix.

7. Concluding remarks

In this paper, a non-destructive approach for parametric identification has been proposed. Based on the analysis of system state behaviour when submitted to a modulated input, a periodic methodology has been presented: forward model, inverse problem, sensitivity analysis, numerical validation, experimental device, experimental validation, and application to isotropic and orthotropic materials. Forward problem is semi-analytically solved thanks to an inverse Fourier transform. For the inverse problem, quadratic criterion describing the difference between simulated and observed phase lags is minimized in order to identify the unknown thermal diffusivities tensor. Robustness of the identification method has been tested, considering several initializations and noisy disturbed observations. Sensitivity analyses have been widely investigated and optimal strategies for the identification of the unknown parameter have been pointed out. It has been shown in orthotropic specific configurations that phase-lag spatial fluctuations at a single frequency are more informative than a frequency sweep at a single point in space. Moreover, in order to minimize the effect of nuisance parameters (such as the Biot number) a suitable excitation frequency range is determined thanks to the reduced sensitivity functions analyses. An experimental device is presented: periodic input is carried out by a heating lamp and an infrared camera is used for modulus and phase-lag observations. Experimental results are shown and assert the measurement bench validation.

Several outlooks can be considered. From the experimental point of view, the foreseeable prejudicial effect of convective heat transfer for low solicitation frequencies has to be carefully taken into account. For the identification method, the iterative algorithm can be modified in order to identify the thermal diffusivity versus z-axis considering phase lag between the heated face centre and the observed face centre. The forward model can be also written using the thermal quadrupoles (Maillet *et al* 2000) in order to characterize multilayered materials. It is also crucial to investigate the confidence of our identification results; the development of interval analysis methods seems to provide an attractive approach (Braems and Jaulin 2001, Jaulin *et al* 2002). Then, based on the presented millimetric experimental device and on a second micrometric device in our institute (Autrique *et al* 2005), a multiscale analysis can be performed in order to better understand, considering orthotropic materials, the relation between local properties of both fibre and matrix and global property of orthotropic sample. Moreover, the analysis of the thermal waves propagation generated by a periodical solicitation could lead to the characterization of the isotropy rate of anisotropic materials such as unidirectional carbon fibres reinforced polymer. In fact, geometric considerations will allow quantifying the rate of fibres liable for the preferential direction of the thermal waves.

Last but not least, both the use of the amplitude of the signal (with an unknown proportionality constant that can be estimated) and the phase can be implemented in a composite criterion to be minimized in order to get a better estimate. This attractive aspect will be investigated in the immediate future.

References

Abou Khachfe R and Jarny Y 2001 Determination of heat sources and heat transfer coefficient for two dimensional heat flow—numerical and experimental study *Int. J. Heat Mass Transfer* **44** 1309–22

Alifanov O M 1994 *Inverse Heat Transfer Problems* (Berlin: Springer) p 348

Angstrom A J 1863 *Phil. Mag.* **25** 130

Autrique L, Perez L and Serra J J 2007 Finite element modelling for microscale thermal investigations using photo thermal microscopy data inversion *Meas. Sci. Technol.* **18** 1–11

Autrique L, Serra J J and Scheer E 2005 Microscale thermal characterization by inverse method in the frequency domain *15th World Congress IFAC (Praha, Czech republic)*

Beck J V and Arnold K J 1977 *Parameter Estimation in Engineering and Science* (New York: Wiley)
Brady G S, Clauser H R and Vaccari J 1997 *Materials Handbook* 14th edn (New York: McGraw-Hill)
Braems I and Jaulin L 2001 Interval analysis for nonlinear parameter and state estimation: contributions and limitations *5th IFAC Symp. on Nonlinear and Control Systems (NOLCOS) (Saint Petersbourg)*
Gill P R, Murray W and Wright M H 1981 *The Levenberg–Marquardt Method. Practical Optimization* (London: Academic Press) pp 136–7
Gurevich Y G, Logvinov G N, de la Cruz G G and Lopez G E 2003 Physics of thermal waves in homogeneous and inhomogeneous (two-layer) samples *Int. J. Therm. Sci.* **42** 63–69
Isakov V 1998 *Inverse Problems for Partial Differential Equations* (Berlin: Springer) p 284
Jaulin L, Braems I, Kieffer M and Walter E 2002 Interval methods for nonlinear identification and robust control *41st IEEE Conf. on Decision and Control (Las Vegas USA)* pp 4676–81
Levenberg K 1944 A method for the solution of certain problems in least squares *Q. Appl. Math.* **2** 164–8
Macedo F, Vaz F, Rebouta L, Carvalho P, Haj-Daoud A, Junge K H, Pelzl J and Bein B K 2008 Modulated IR radiometry of (TiSi)N thin films *Vacuum* **82** 1457–60
Maillet D, André S, Batsale J C, Degiovanni A and Moyne C 2000 *Thermal Quadrupoles, Solving the Heat Equation through Integral Transforms* (Chichester: Wiley)
Marquardt D 1963 An algorithm for least-squares estimation of nonlinear parameters *SIAM J. Appl. Math.* **11** 431–41
Montgomery D C 1997 *Design and Analysis of Experiments* (New York: Wiley)
Muscio A, Bison P G, Marinetti S and Grinzato E 2004 Thermal diffusivity measurement in slabs using harmonic and one-dimensional propagation of thermal waves *Int. J. Therm. Sci.* **43** 453–63
Rouquette S, Autrique L, Chaussavoine C and Thomas L 2007 Identification of influence factors in a thermal model a plasma assisted chemical vapour deposition process *Inverse Problems Sci. Eng.* **15**
Venerus D C, Schieber J D, Iddir H, Guzman J D and Broerman A W 1999 Measurement of thermal diffusivity in polymer melts using forced Rayleigh light scattering *J. Polym. Sci.* B **37** 1069–78
Walter E and Pronzato L 1997 *Identification of Parametric Models from Experimental Data* (Berlin: Springer)